Earth and Planetary Science Letters 365 (2013) 177–189

Contents lists available at SciVerse ScienceDirect

Earth and Planetary Science Letters

journal homepage: www.elsevier.com/locate/epsl

The stable vanadium isotope composition of the mantle and mafic lavas

J. Prytulak [a,b,*], S.G. Nielsen [b,c], D.A. Ionov [d], A.N. Halliday [b], J. Harvey [e], K.A. Kelley [f], Y.L. Niu [g], D.W. Peate [h], K. Shimizu [i], K.W.W. Sims [j]

[a] Department of Earth Science and Engineering, Imperial College London, London SW7 2AZ, UK
[b] Department of Earth Sciences, University of Oxford, South Parks Road, Oxford OX1 3AN, UK
[c] Department of Geology & Geophysics, Woods Hole Oceanographic Institute, 266 Woods Hole, MA 02543-1050, USA
[d] Université de Saint Etienne & UMR6524-CNRS, F-42023, France
[e] School of Earth and Environment, University of Leeds, Leeds LS2 9JT, UK
[f] Graduate School of Oceanography, University of Rhode Island, RI 02882-1197, USA
[g] Department of Earth Science, University of Durham, Durham DH1 3LE, UK
[h] Department of Geosciences, University of Iowa, IA 52242, USA
[i] Institute for Research on Earth Evolution, Japan Agency of Marine-Earth Science and Technology, 2-15 Natsushima, Yokosuka 237-001, Japan
[j] Department of Geology and Geophysics, University of Wyoming, USA

ARTICLE INFO

Article history:
Received 10 August 2012
Received in revised form
4 January 2013
Accepted 11 January 2013
Editor: B. Marty

Keywords:
vanadium isotopes
bulk silicate Earth
high temperature stable isotope
fractionation

ABSTRACT

Vanadium exists in multiple valence states under terrestrial conditions (2^+, 3^+, 4^+, 5^+) and its isotopic composition in magmas potentially reflects the oxidation state of their mantle source. We present the first stable vanadium isotope measurements of 64 samples of well-characterized mantle-derived mafic and ultramafic rocks from diverse localities. The δ^{51}V ranges from −0.27‰ to −1.29‰, reported relative to an Alfa Aesar (AA) vanadium solution standard defined as 0‰. This dataset is used to assess the effects of alteration, examine co-variation with other geochemical characteristics and define a value for the bulk silicate Earth (BSE). Variably serpentinised peridotites show no resolvable alteration-induced δ^{51}V fractionation. Likewise, altered mafic oceanic crustal rocks have identical δ^{51}V to fresh hand-picked MORB glass. Intense seafloor weathering can result in slightly (~0.2–0.3‰) heavier isotope compositions, possibly related to late-stage addition of vanadium. The robustness of δ^{51}V to common alteration processes bodes well for its potential application to ancient mafic material. The average δ^{51}V of mafic lavas, including MORB, Icelandic tholeiites and lavas from the Shatsky Rise large igneous province is -0.88 ± 0.27‰ 2sd. Peridotites show a large range in primary δ^{51}V (−0.62‰ to −1.17‰), which co-varies positively with vanadium concentrations and indices of fertility such as Al_2O_3. Although these data suggest preferential extraction of heavier isotopes during partial melting, the isotope composition of basalts ($\delta^{51}V = -0.88 \pm 0.27$‰ 2sd) and MORB glass in particular ($\delta^{51}V = -0.95 \pm 0.13$‰ 2sd) is lighter than fertile peridotites and thus difficult to reconcile with a melt extraction scenario. Determination of fractionation factors between melt and mineral phases such as pyroxenes and garnet are necessary to fully understand the correlation. We arrive at an estimate of $\delta^{51}V_{BSE} = -0.7 \pm 0.2$‰ (2sd) for the bulk silicate Earth by averaging fertile, unmetasomatised peridotites. This provides a benchmark for both high and low temperature applications addressing planet formation, cosmochemical comparisons of the Earth and extraterrestrial material, and an inorganic baseline for future biogeochemical investigations. Whilst δ^{51}V could relate to oxidation state and thus oxygen fugacity, further work is required to resolve the isotopic effects of oxidation state, partial melting, and mineral fractionation factors.

1. Introduction

Radiogenic isotopic compositions measured in mantle rocks and mantle-derived magmas provide compelling evidence for the existence of mantle heterogeneity as well as constraints on its creation and preservation (e.g., Hofmann, 2003; Zindler and Hart, 1986). However, long-lived radiogenic isotope signatures are not without ambiguity. The variability in isotopic compositions of Sr, Nd, Pb, and Hf, for example, reflects the time-integrated fractionation of parent from daughter element. The magnitude of this elemental fractionation, the initial source composition and the age of the fractionated material all contribute to uncertainty in interpreting the final isotope composition. Thus, deducing the

* Corresponding author at: Department of Earth Science and Engineering, Imperial College London, London, SW7 2AZ, UK. Tel.: +44 207 954 6474.
E-mail address: j.prytulak@imperial.ac.uk (J. Prytulak).

0012-821X/$ - see front matter © 2013 Elsevier B.V. All rights reserved.
http://dx.doi.org/10.1016/j.epsl.2013.01.010

often multi-stage journey of the mantle and its melts is inherently non-unique using radiogenic isotopes.

Stable isotopes offer valuable complementary information to the evidence provided by long-lived radiogenic isotopes; particularly since neither time nor parent–daughter fractionations need be considered. Instead stable isotope fractionation is driven by temperature related equilibrium fractionations, relative mass differences, bond strengths, and kinetic processes (see review by Schauble, 2004). Of particular interest is the inverse relationship between temperature and magnitude of isotope fractionation (Urey, 1947). Since isotope fractionation at high temperatures was, until recently, considered negligible, stable isotope variability in the mantle or its melts has been attributed to the recycling and incorporation of surface material. Oxygen and sulphur isotopes have long been used in this manner to deduce the presence of sedimentary or hydrothermally altered material in the source of mantle melts (e.g., Chaussidon et al., 1987; Eiler et al., 1996). However, oxygen is a major constituent of the mantle, so large amounts of material are needed to impact oxygen isotope signatures. Sulphur isotopes are generally measured on sulphides and can show large isotope fractionations (e.g., Chaussidon et al., 1987; Bekker et al., 2009). However, sulphides are not always present in samples of interest, and the susceptibility of sulphur to volatile, degassing-driven isotope fractionation is a concern in erupted lavas. So-called 'non-traditional' stable isotopes have become increasingly prevalent in mantle studies.

For example, stable isotope systems of elements such as lithium (e.g., Elliott et al., 2006) and thallium (e.g., Nielsen et al., 2006) have been employed to trace small contributions of surface materials into the source of mantle-derived melts.

Advances in multi-collector inductively coupled plasma mass spectrometry (MC-ICPMS) technology have greatly improved analytical precision, facilitating the exploration of small variations in stable isotopes at high temperatures of elements traversing the entire periodic table (e.g., Halliday et al., 2010). Research has focused on teasing out the causes of ubiquitous non-traditional stable isotope fractionation and applying this new information to geologic questions. This task is aided by resurgence in theoretical consideration of high temperature stable isotope fractionation after a long period with little work (e.g., Bigeleisen and Mayer, 1947; Schauble, 2004, Schauble et al., 2001, 2009; Urey, 1947). In particular, isotope systems of the period four transition metal elements are being increasingly studied. Multiple oxidation states of some transition metals and the prediction that changes between oxidation states can be linked to isotope fractionation (e.g., Schauble, 2004) means that transition metal stable isotopes potentially provide key information about, for example, the physical conditions of a mantle source (e.g., oxygen fugacity) rather than simply a test for crustal recycling.

Iron isotopes were amongst the first transition metal to have been investigated for high temperature fractionation (e.g., Zhu et al., 2000) and thus are perhaps currently the best understood. High temperature iron isotopic fractionation has been linked to changing oxygen fugacity (e.g., Dauphas et al., 2009; Williams et al., 2004, 2005), magmatic differentiation (Hibbert et al., 2012; Schuessler et al., 2009; Teng et al., 2008; Weyer and Ionov, 2007; Williams et al., 2004, 2005) and diffusion (Teng et al., 2011; Weyer and Seitz, 2012). Far fewer data are available for chromium stable isotopes at high temperatures, with initial results indicating negligible fractionation in major terrestrial reservoirs (Schoenberg et al., 2008). Hence, it is still unclear if the redox behaviour of transition metal isotopes provides new, robust proxies for mantle oxygen fugacity.

We have developed the first method able to measure stable vanadium isotopes to a precision useful for geologic problems (Nielsen et al., 2011a; Prytulak et al., 2011). Here we present the first investigation of vanadium isotopes in mafic and ultramafic igneous rocks in order to determine the applicability of vanadium isotopes to mantle processes.

1.1. Vanadium and vanadium isotopes: applications and aims

Vanadium is a moderately incompatible, refractory transition metal existing in multiple valence states (V^{2+}, V^{3+}, V^{4+}, V^{5+}) at terrestrial conditions. Many studies have taken advantage of redox properties of vanadium and the strong relationship between vanadium partitioning and oxygen fugacity (e.g., Canil, 1997). These include investigation of the oxidation state of the mantle through time (e.g., Lee et al., 2003; Li and Lee, 2004), the oxidation state of subduction zones (e.g., Lee et al., 2005), core formation (e.g., Wood et al., 2008), oceanic anoxia (e.g., Emerson and Huested, 1991; Tribovillard et al., 2006), hydrocarbon and crude oil genesis (e.g., Lopez et al., 1995), and nitrogen fixation (e.g., Bellenger et al., 2008). Whilst useful, elemental studies are prone to uncertainties such as initial source concentration, degree of melting and partitioning relationships. Stable isotopes may provide more straightforward information.

Changes in oxidation state are theoretically predicted, and experimentally demonstrated to result in fractionation of stable isotopes (e.g., Schauble et al., 2009; Urey, 1947; Zhu et al., 2000). Vanadium may be particularly advantageous in this respect given the number of oxidation states available. Considering the large array of potential applications to problems in Earth science, it might be surprising that to date no high precision vanadium isotope data exist. This lack of vanadium isotope data is due to two major analytical obstacles. The first is that the $^{51}V/^{50}V$ of the only two stable isotopes, ^{51}V (99.76%) and ^{50}V (0.24%), is $\sim$420. The analytical challenge is compounded by the existence of direct isobaric interferences from ^{50}Cr and ^{50}Ti on the minor ^{50}V isotope. The first separation and measurement protocol that overcomes these difficulties for silicate matrices has been developed (Nielsen et al., 2011a; Prytulak et al., 2011). This study presents the first investigation of high temperature fractionation of stable vanadium isotopes in mantle and mantle-derived mafic melts with three general aims

1) Evaluate the range of natural isotope fractionation in the mantle and mafic mantle-derived melts
2) Assess the fidelity of the isotope signature to common alteration processes
3) Estimate the stable vanadium isotope signature of the bulk silicate Earth.

2. Materials

Exploration of new isotope systems is hindered without basic geochemical context. Therefore bulk rock major elements are the minimum characterization requirement for the samples in this study. Trace element and isotopic data are also available in most cases. Every effort has been made to investigate samples previously studied for other 'non-traditional' stable isotope systems (e.g., Li, Mg, Fe, and Cr). Full major and trace element characterization and GPS locations (where available) for the 64 samples in this study can be found in the literature, and is also compiled in the Electronic Appendix. A supplemental figure is included with the global locations of all samples in this study.

2.1. Fresh and altered peridotites

Twenty-four peridotites were chosen from a variety of locations and targeted to include a range of melt depletion and degrees of alteration. Abyssal peridotites from Ocean Drilling Program (ODP) Leg 209, Site 1274A in the North Atlantic are some of the most melt depleted recovered thus far (20–30%, Bach et al., 2004; Harvey et al., 2006). They are extensively and systematically altered, with serpentinisation intensity increasing with depth below the seafloor. Nine dredged abyssal peridotites from the South West Indian Ridge, American-Antarctic Ridge, and the Pacific-Antarctic Ridge are presented (Niu, 2004). The dredged abyssal peridotites have been extensively serpentinised and subjected to low temperature seafloor weathering.

In an attempt to sample more pristine mantle material, we measured peridotite xenoliths from several continental localities. These include spinel and garnet lherzolites from East Africa (Dawson et al., 1970), Mongolia (Ionov and Hofmann, 2007) and Siberia (Ionov, 2004; Ionov et al., 1993). The peridotites include fertile samples previously used to assess the Fe, Li and Mg isotopic compositions of the bulk silicate Earth (Pogge von Strandmann et al., 2011; Weyer and Ionov, 2007). Finally, we include analyses of USGS dunite standard DTS and PCC1. δ^{51}V of PCC1 is from Prytulak et al. (2011).

2.2. Fresh and altered MORB

Six fresh, hand-picked MORB glass samples from the Indian Ocean (Gannoun et al., 2007) and the Kolbeinsey Ridge (Elkins et al., 2011) are presented in addition to composite MORB from ODP Leg 185 Hole 801C in the Pacific Ocean. The composite samples are physical mixtures of lava from different intervals in the drill core. They were constructed using visual estimates of lithologic units, coupled with natural gamma and formation microscanner logs from shipboard measurements. We present measurements of MORB composites from different depths in Hole 801C and a 'SUPER' composite which was constructed to represent the entire subducting package, including intercalated sediments, at ODP Hole 801C. Detailed discussion of the composite sampling strategy is given in Plank et al. (2000), and specific core intervals used for their construction plus major and trace element data is found in Kelley et al. (2003). Since composites identify large-scale changes in geochemistry, we complement them with 12 discrete samples from drill sites 801B, C, 1149B, C, and D from ODP Legs 129 and 185 (Kelley et al., 2003) all outboard of the Izu–Bonin–Mariana trench on crust ranging from 135 to 170 Ma in age.

2.3. Other mantle-derived 'OIB' mafic lavas

To represent primitive mantle-derived lavas other than MORB, we include USGS standards BCR2 (Columbia River flood basalt), BHVO1 and 2 (Hawaiian basalt), BIR1a (Icelandic basalt) that have previously reported δ^{51}V (Prytulak et al., 2011). We augment these rock standards with mantle-derived material from two other locations.

The first is a suite of nine historic, mafic, sparsely phyric ($<5\%$) tholeiitic basalts from the Reykjanes peninsula, Iceland (Peate et al., 2009). The second suite consists of four well-characterized glassy basalts from the Shatsky Rise large igneous province, drilled by IODP Expedition 324 (Sager et al., 2010). Four main magma types were recovered on Shatsky: 'normal', low-Ti, high-Nb, and 'U1349-type' (Sano et al., 2012). The 'normal' lava type is similar to N-MORB in chemical compositions and the most voluminous on Shatsky, therefore we present two 'normal' lavas for comparison with a low-Ti and high-Nb lava.

3. Methods

The vanadium isotope chemical separation and measurement protocol is fully described in Nielsen et al. (2011a) and Prytulak et al. (2011). Here we briefly highlight some sample-specific issues.

3.1. Sample digestion

Two types of sample digestion were employed. Peridotites contain refractory spinel that cannot be dissolved by standard hotplate techniques. To ensure complete dissolution, peridotites were dissolved using mini-teflon hexagonal screw-top bombs. Approximately 70 mg of sample was dissolved in 2:1 mixture of 29 M HF:14 M HNO_3 and placed in an oven at 140 °C for 3 days. Samples were visually assessed for dissolution (spinel appeared as small black particles). If spinel was visible, then the sample was bombed again for 4 days in 1:1 10 M HCl+29 M HF. After this stage samples always achieved full dissolution.

Standard hotplate methods were sufficient to completely dissolve mafic lavas. Lava samples were dissolved in a mixture of 5:1 29 M HF:14 M HNO_3 at 160 °C on a hotplate for at least 24 h. They were then evaporated with 14 M HNO_3 three times at 160 °C to destroy fluorides formed from the initial dissolution.

3.2. Peridotite considerations

Between 5 and 10 μg of vanadium is required for repeat measurements. This does not present an issue for the lavas with V concentrations in excess of 100 μg g^{-1}. However, depleted peridotites pose a greater challenge. The chemical separation procedure is only effective to <100 mg of processed sample. The low V concentration of peridotites (down to $\sim$10 μg g^{-1}V) necessitated several digestions of the same powder to be independently passed through the first three stages of chemical separation, then re-combined for the final removal of Cr and Ti (see Nielsen et al., 2011a). Since peridotites contain on the order of several 1000 μg g^{-1} Cr, a Cr cleanup column was repeated three times to achieve adequate removal of Cr for precise measurements (see also Prytulak et al., 2011).

3.3. MC-ICPMS

Measurement protocols are fully described in Nielsen et al. (2011a) and Prytulak et al. (2011), but we briefly recap the salient details. Measurements were performed on Nu Plasma HR-MC-ICP-MS (Nu Instruments, Wrexham, UK) instruments at the University of Oxford and Imperial College London. The Oxford instrument has a non-standard collector configuration (see Nielsen et al., 2011a).

The ratio of $^{51}V/^{50}V$ is $\sim$420, therefore V measurements employ a 10^9 Ω resistor on the Faraday cup collecting ^{51}V, with all other Faraday cups using standard 10^{11} Ω resistors. Samples were measured using a sample-standard bracketing method in 0.1 M HNO_3 for one block of 40 ratios. Vanadium isotopes are reported using standard delta notation:

$$\delta^{51}V = 1000 \times [(^{51}V/^{50}V_{sample}/^{51}V/^{50}V_{AA})-1]$$

The Alfa Aesar (AA) V standard solution is defined as $\delta^{51}V=0‰$ (Nielsen et al., 2011a). A secondary V standard solution from BDH chemicals is used to evaluate machine performance. The long-term isotope composition of BDH (2009–2012) run at Oxford University is $-1.18 \pm 0.17‰$ 2sd ($n=877$) and at Imperial College London is $-1.19 \pm 0.17‰$ 2sd ($n=452$). Total procedural blanks at both Oxford and Imperial were <2 ng, which is negligible compared to the total amount of V processed (5–25 μg).

Table 1
Stable vanadium isotope compositions.

Sample	Rock type	V ($\mu g\,g^{-1}$)	$\delta^{51}V$	2σ	Dissolutions	Runs	Sessions	Institution	Sample reference
Peridotites									
313-1	Gnt Lherz	NA	−0.72	NA	1	1	1	IC	Ionov et al. (1993)
313-6	Gnt Lherz	109	−0.62	NA	1	1	1	IC	Ionov et al. (1993)
313-102	Gnt Lherz	100	−0.58	0.07	1	2	1	IC	Ionov (2004)
313-104	Gnt Lherz	88	−0.83	0.22	2	6	2	IC	Ionov (2004)
313-106	Gnt Lherz	75	−0.75	0.03	1	2	1	IC	Ionov (2004)
313-112	Gnt Lherz	105	−0.70	NA	1	1	1	IC	Ionov (2004)
BD 730	Gnt Lherz	41	−0.99	0.20	1	4	1	Oxford	Dawson et al. (1970)
BD 822	Sp Lherz	13	−0.78	NA	1	1	1	Oxford	Dawson et al. (1970)
314-56	Sp Lherz	NA	−0.77	NA	1	1	1	IC	Ionov et al. (1993)
314-58	Sp Lherz	NA	−0.81	0.29	2	3	1	IC	Ionov et al. (1993)
Mo 101	Sp Lherz	NA	−0.64	0.09	1	3	1	IC	Ionov and Hofmann (2007)
RC27-9 34-33	Abys. peridotite	63	−0.84	0.14	1	5	2	IC	Niu (2004)
PROT 40D-54	Abys. peridotite	55	−0.27	0.24	2	7	4	Oxford and IC	Niu (2004)
PROT 15D-35	Abys. peridotite	51	−0.69	0.13	2	8	3	Oxford and IC	Niu (2004)
PROT 13D-46	Abys. peridotite	30	−0.66	0.24	2	3	2	Oxford and IC	Niu (2004)
PROT 5 38-1	Abys. peridotite	46	−0.78	0.12	1	5	2	Oxford and IC	Niu (2004)
www3 13D-5-2	Abys. peridotite	59	−0.80	0.01	1	2	1	Oxford	Niu (2004)
Vulcan 5 41-29	Abys. peridotite	61	−0.74	0.15	1	3	1	Oxford	Niu (2004)
Vulcan 5 41-55	Abys. peridotite	59	−0.44	0.24	1	5	2	Oxford and IC	Niu (2004)
Vulcan 5 35-3	Abys. peridotite	32	−0.84	0.08	1	5	2	Oxford and IC	Niu (2004)
1274A-5R2-25-35	Harzburgite	29	−1.17	0.07	1	3	1	Oxford	Harvey et al. (2006)
1274A-11R1-56-65	Harzburgite	26	−1.17	0.10	1	4	1	Oxford	Harvey et al. (2006)
1274A-27R1-130-140	Harzburgite	19	−1.08	0.07	1	3	1	Oxford	Harvey et al. (2006)
1274A-5R2-25-35[a]	*Harzburgite*	*29*	*−1.32*[a]	*0.14*[a]	*1*	*6*	*1*	*Oxford*	Harvey et al. (2006)
1274A-27R1-130-140[a]	*Harzburgite*	*19*	*−1.25*[a]	*0.18*[a]	*1*	*5*	*1*	*Oxford*	Harvey et al. (2006)
MORB glass									
POS210/1	Basalt	291	−0.97	0.22	2	12	5	Oxford and IC	Elkins et al. (2011)
TR 6D 2g	Basalt	393	−0.92	0.01	1	2	1	Oxford	Elkins et al. (2011)
TR30D 2g	Basalt	291	−0.96	0.05	1	3	3	Oxford	Elkins et al. (2011)
TR 16D 1g	Basalt	399	−1.04	0.15	1	6	3	Oxford	Elkins et al. (2011)
TR 15D 1g	Basalt	329	−0.84	0.15	1	3	1	Oxford	Elkins et al. (2011)
MD57	Basalt	316	−0.99	0.09	1	6	3	Oxford	Gannoun et al. (2007)
MORB composites ODP Hole 801C									
MORB 0-110	Composite	251	−0.90	0.17	1	2	2	Oxford	Kelley et al. (2003)
MORB 110-220	Composite	399	−0.97	0.09	1	4	2	Oxford	Kelley et al. (2003)
MORB 220-420 FLO	Composite	399	−0.97	0.20	1	5	2	Oxford	Kelley et al. (2003)
801 SUPER	Composite	338	−0.89	0.18	1	3	2	Oxford	Kelley et al. (2003)
Discrete altered oceanic crust samples									
1149B 30R2 56-62	Alt. basalt+cc vein and halo	337	−0.81	0.04	1	3	1	Oxford	Kelley et al. (2003)
1149C 10R2 47-51	Basalt	358	−0.81	0.17	2	6	3	Oxford	Kelley et al. (2003)
1149D 7R1 37-41	Hyaloclastite	64	−1.16	NA	1	1	1	Oxford	Kelley et al. (2003)
1149D 9R3 30-32	Alt. basalt+halo	324	−0.92	0.26	1	6	3	Oxford	Kelley et al. (2003)

1149D 11R2 86-92	Breccia of basalt+cc cement	194	−0.78	0.10	1	2	2	Oxford	Kelley et al. (2003)
1149D 16R3 2-8	Basalt	307	−0.71	0.09	1	2	1	Oxford	Kelley et al. (2003)
1149D 17R1 92-98	Basalt+cc veins	235	−0.93	0.10	1	3	2	Oxford	Kelley et al. (2003)
1149D 19R1 85-89	Basalt	415	−0.83	0.06	1	2	1	Oxford	Kelley et al. (2003)
801B 43R1 132-135	Basalt	173	−0.65	NA	1	1	1	Oxford	Kelley et al. (2003)
801C 15R7 31-34	Alt. basalt	433	−1.04	0.17	1	3	1	Oxford	Kelley et al. (2003)
801C 34R1 93-96	Basalt+FeOx vein and halo	442	−0.93	0.23	1	4	3	Oxford	Kelley et al. (2003)
801C 44R3 23-26	Basalt+cc veins and haloes	410	−0.82	0.20	1	3	3	Oxford	Kelley et al. (2003)
Recent Icelandic tholeiites									
408673	Tholeiitic basalt	467	−0.94	0.06	1	3	2	Oxford	Peate et al. (2009)
4567 14	Tholeiitic basalt	374	−0.82	0.12	1	4	1	Oxford	Peate et al. (2009)
4567 22	Tholeiitic basalt	423	−0.75	0.26	1	4	1	Oxford	Peate et al. (2009)
4567 32	Tholeiitic basalt	339	−0.88	0.14	2	8	1	Oxford	Peate et al. (2009)
4567 36	Tholeiitic basalt	342	−0.80	0.21	1	5	1	Oxford	Peate et al. (2009)
4567 40	Tholeiitic basalt	359	−0.85	0.10	1	5	2	Oxford	Peate et al. (2009)
4567 43	Tholeiitic basalt	351	−0.82	0.27	1	4	3	Oxford	Peate et al. (2009)
4567 45	Tholeiitic basalt	376	−1.00	0.07	1	3	2	Oxford	Peate et al. (2009)
4567 49	Tholeiitic basalt	279	−0.93	NA	1	1	1	Oxford	Peate et al. (2009)
Shatsky rise basalts IODP Exp. 324									
U1347A-17R-2-4/8	Low Ti′ basalt	428	−0.69	0.02	1	3	1	IC	Sano et al. (2012)
U1350A-17R-2-126/129	High Nb′ basalt	357	−1.29	0.31	1	3	1	IC	Sano et al. (2012)
U1350A-22R-2-122/124	'Normal' basalt	289	−0.66	0.09	1	3	1	IC	Sano et al. (2012)
U1350A-24R-2-110/113	'Normal' basalt	274	−0.70	0.23	1	3	1	IC	Sano et al. (2012)
USGS basalts and peridotites									
BIR1a	Icelandic basalt	310	−0.92	0.16	12	50	8	Oxford	USGS website
BHVO1	Hawaiian basalt	317	−0.92	0.04	1	4	1	Oxford	USGS website
BHVO2	Hawaiian basalt	317	−0.88	0.10	7	14	4	Oxford	USGS website
BCR2	CR flood basalt	416	−0.92	0.16	13	27	7	Oxford	USGS website
DTS	Dunite	11	−0.95	NA	1	1	1	Oxford	USGS website
PCC1	Dunite	31	−1.01	0.09	2	8	3	Oxford	USGS website
PCC1[a]	*Dunite*	*31*	*−1.29*[a]	*0.21*	*5*	*10*	*3*	*Oxford*	USGS website

'Dissolutions' refers to the number of complete repeat digestions and chemical separations of a sample; 'Runs' refers to the number of individual sample measurements made for that sample; and 'Sessions' refers to the number of separate mass spectrometry sessions (often separated by weeks), that the same sample was run in. *Note*: 2σ of sample is the internal error if only one dissolution was performed. The 2σ of samples with multiple dissolutions is the external reproducibility. NA=data not available, or the sample was only run once and an error of ± 0.17‰ is used for figures. IC=Imperial College London.

[a] Samples with residual spinel.

4. Results

The range of δ^{51}V for the 64 samples is −0.27‰ to 1.29‰ (Table 1). We consider the long-term reproducibility of our BDH V solution standard (0.17‰) to be the best currently achievable measurement precision. Therefore, in all subsequent figures, samples with 2sd < 0.17‰, or those that could only be run once, employ error bars of 0.17‰, whilst the actual sample 2sd is used when > 0.17‰.

Peridotites display the largest isotopic variation, with δ^{51}V from −0.27‰ to −1.17‰ (n=23). In contrast, fresh MORB glass has a more restricted isotopic range of −0.84‰ to −1.04‰ (n=6). Composite samples from altered oceanic crust (AOC) at ODP Hole 801C are similarly restricted with δ^{51}V of −0.89‰ to −0.97‰ (n=4). Discrete AOC samples from ODP Hole 801C do not differ significantly from MORB glasses and AOC composites with a range of −0.65‰ to −1.16‰ (n=12). The average of all fresh MORB and AOC composites is -0.95 ± 0.11‰ 2sd (n=9).

Other mafic lavas include a suite of tholeiites from the Rekyjanes peninsula with δ^{51}V= −0.75 to −1.00 (n=8) and an average of -0.86 ± 0.15‰ 2sd, also similar to MORB. The four basalts from the Shatsky Rise show more variation, with a range of δ^{51}V from −0.66‰ to −1.29‰.

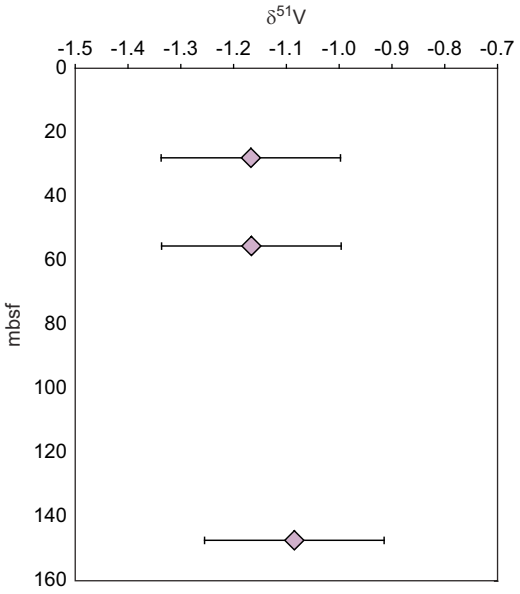

Fig. 1. Stable vanadium isotope composition of abyssal peridotites from ODP Hole 1274A (Harvey et al., 2006) versus depth in metres below sea floor (mbsf).

5. Discussion

We first discuss the effects of common alteration processes on δ^{51}V of peridotites and mafic rocks. Secondly, we assess the impact of partial melting, mineral modes and differentiation. Lastly, we evaluate the δ^{51}V composition of the bulk silicate Earth.

5.1. Alteration of primary δ^{51}V signatures

It is desirable to determine how robust δ^{51}V is to common secondary processes such as hydrothermal alteration, serpentinisation and seafloor weathering. Three suites were chosen for investigation, including (1) systematically serpentinised abyssal peridotites (Bach et al., 2004; Harvey et al., 2006), (2) abyssal peridotites that have experienced extensive seafloor weathering (Niu, 2004), and (3) composite and discrete AOC from ODP Leg 129 and 185 (Kelley et al., 2003).

5.1.1. Serpentinisation of ODP Leg 209 abyssal peridotites

Serpentinisation most drastically affects olivine. Vanadium does not strongly partition into olivine and therefore we predict that δ^{51}V remains robust to serpentinisation. Furthermore, serpentinisation is largely isochemical (with the exception of water, Komor et al., 1985), and thus the opportunity for isotopic fractionation is limited. To distinguish the effects of serpentinisation versus seafloor weathering (Section 5.1.2) we use drill core samples without prolonged exposure to seawater. We measured three abyssal harzburgites from ODP Leg 209, which display variable degrees of serpentinisation from ~60% to 100% (Bach et al., 2004; Harvey et al., 2006). We find no δ^{51}V fractionation associated with the degree of serpentinisation (Fig. 1).

5.1.2. Seafloor weathering of dredged abyssal peridotites

'Seafloor weathering' can significantly affect the primary chemical composition of abyssal peridotites. It occurs at temperatures < 150 °C, and is typified by Mg loss and alkali element enrichment, although the two are not necessarily directly linked (Snow and Dick, 1995). As with serpentinisation, V abundances are largely immune to seafloor weathering. Such a process may result in slight V enrichment, possibly explained by artificial inflation due to Mg loss (Snow and Dick, 1995).

To test the effects of seafloor weathering on δ^{51}V, we measured nine extensively altered dredged abyssal peridotites (Niu, 2004). These samples are from various locations in the Pacific and Indian oceans and therefore can inform on general processes, but cannot be used to evaluate the extent of alteration in individual localities. Additionally, the size of the samples is small (1–2 cm), which amplifies variation due to mineralogical heterogeneity. Despite these caveats, vanadium and scandium abundances in the sample set of Niu (2004), which includes ~130 abyssal peridotites, retain systematic co-variation with MgO, which may be indicative of primary melt extraction trends (Niu, 2004).

The stable vanadium isotope composition of nine dredged peridotites from Niu (2004) span the largest range within a single suite (−0.29‰ to −0.84‰). There is no correlation of δ^{51}V with Al_2O_3 or TiO_2 contents that may suggest melt extraction (Fig. 2a and b). If anything, it appears that the most depleted (i.e. lowest TiO_2 and Al_2O_3) samples are the most variable, which could be consistent with refertilisation of a V-depleted peridotite. Furthermore, the rocks with the highest V contents display the largest range in δ^{51}V (Fig. 2c). However, this relationship could also be a facet of different melt extraction histories, initial compositions and late stage percolation in melting residues. Slightly more informative is the diffuse positive relationship of δ^{51}V with Sr and Ba (Fig. 2d and e), elements that are enriched by seafloor weathering. Therefore, although the effect remains ambiguous, it appears that extreme seafloor weathering may drive δ^{51}V slightly heavier by 0.2–0.3‰. We consider the heaviest δ^{51}V for abyssal peridotite (δ^{51}V= -0.29 ± 0.24‰), which also displays the highest Ba and Sr contents and the lowest TiO_2 and Al_2O_3 contents, unlikely to be primary. However, a detailed study requires a co-genetic suite where the effects of source composition, melt extraction and post-melting processes can be independently assessed.

5.1.3. $\delta^{51}V_{MORB}$ and low temperature alteration of mafic oceanic crust

Understanding chemical changes occurring in the mafic oceanic crust during hydrothermal alteration is critical to evaluating chemical fluxes to the ocean and the budgets of elements that are recycled into the deeper mantle (see review by Staudigel, 2003).

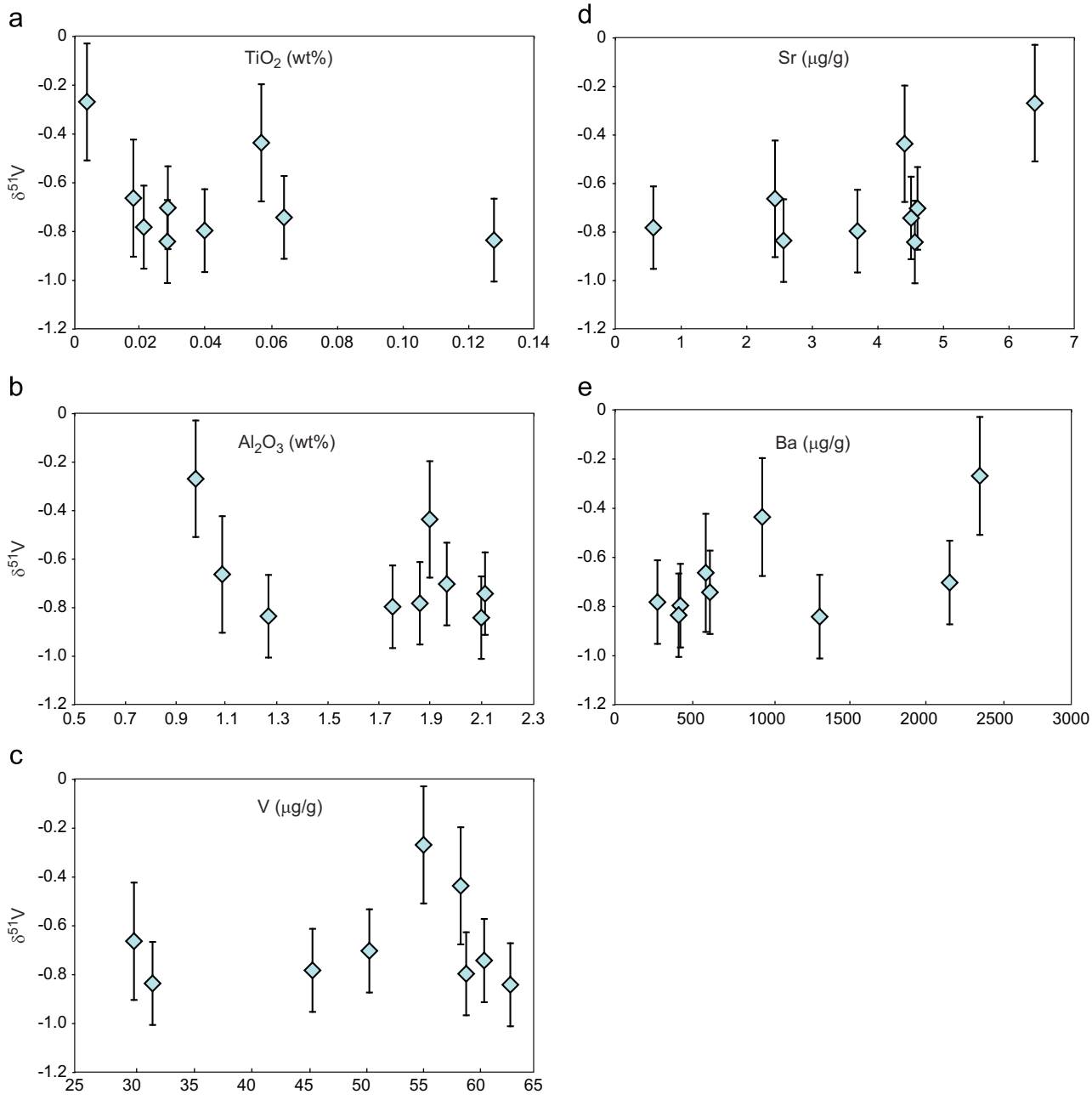

Fig. 2. Stable vanadium isotope composition of dredged abyssal peridotites from Niu (2004) versus (a) TiO_2, (b) Al_2O_3, (c) V, (d) Sr, and (e) Ba.

Furthermore, ancient mafic crust likely underwent similar processes, and therefore we require knowledge of how faithfully $\delta^{51}V$ retains its initial signature in order to apply the technique to ancient samples. To this end, we compare $\delta^{51}V$ in fresh MORB glass with composites and discrete samples of altered oceanic crust (Table 1). As with serpentinisation and seafloor weathering, there is little evidence for elemental V addition or removal during low temperature hydrothermal alteration (e.g., Kelley et al., 2003). Vanadium is removed from seawater by particulate scavenging in high temperature hydrothermal plumes above mid-ocean vents (e.g., Elderfield and Schultz, 1996). However, there is no evidence that seawater alteration introduces vanadium into the ocean crust.

Fig. 3 compares fresh MORB glass from the Indian Ocean and Kolbeinsey Ridge with altered oceanic crust (AOC) composites from ODP Hole 801C in the Pacific Ocean including a 'SUPER' composite representative of the entire subducting package of sediments and mafic crust (Kelley et al., 2003). There is remarkably little variation in the basalts, with an average $\delta^{51}V$ of -0.95 ± 0.11‰ 2sd ($n=9$) spanning vanadium contents of $\sim$250–400 μg g^{-1}.

Analyses of the composites provide averaged chemical compositions over $\sim$100 m of drill core. Therefore it is also important to investigate the $\delta^{51}V$ of discrete intervals from ODP Holes 801B, C and Hole 1149B, C, and D. These samples are advantageous in that some have been studied for Fe isotopes (Rouxel et al., 2003) and allow initial comparison of $\delta^{51}V$ with another redox sensitive transition metal stable isotope system. Kelley et al. (2003) evaluated chemical enrichments and depletions in drill samples from Legs 129 and 185. The most significant change was a ninefold enrichment in rubidium (Rb). The lightest $\delta^{51}V$ value of -1.16‰ is found in a hyaloclastite with significant Rb

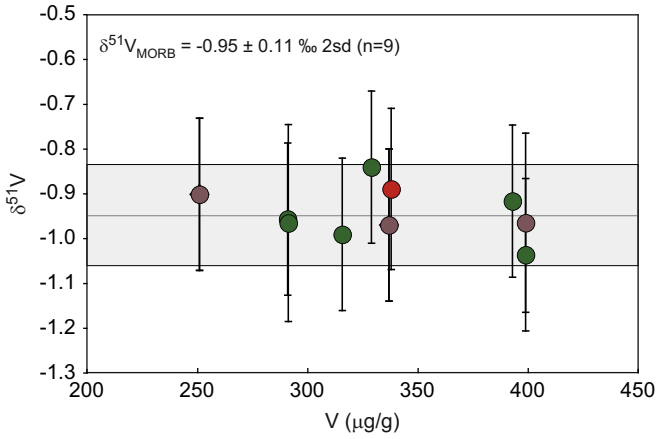

Fig. 3. Stable vanadium isotope composition of fresh and altered MORB versus vanadium content. Fresh MORB: green circles; altered MORB composites: brown circles; SUPER composite (see text): red circle. (For interpretation of the references to colour in this figure legend, the reader is referred to the web version of this article.)

enrichment (51 $\mu g\,g^{-1}$ versus an average of 12 $\mu g\,g^{-1}$ in the other discrete samples) and notable V depletion compared to the other discrete samples (64 $\mu g\,g^{-1}$ at 8.9 wt% MgO). This sample clearly invites a more focused study on the extent of high and low temperature hydrothermally induced V isotope fractionation. However, even with the inclusion of the hyaloclastite, there is little overall variation in the discrete AOC suite (Table 1), despite their differing extents and types of alteration (see Kelley et al., 2003). The discrete AOC average $\delta^{51}V$ (excluding the hyaloclastite) is -0.84 ± 0.22‰ 2sd, overlapping with the range seen in MORB glass and AOC composites. Thus $\delta^{51}V$ appears generally insensitive to common low temperature alteration processes occurring in the mafic oceanic crust.

Iron isotopes have been touted as a potential tool to examine past oxidation conditions in igneous materials (e.g., Dauphas et al., 2009, 2010). It is therefore useful to make some initial comparisons of the $\delta^{51}V$ homogeneity with the range of Fe isotope values documented in the same drill cores. Rouxel et al. (2003) found a large total range in $\delta^{57}Fe$ outside their analytical error of 0.2‰. Positive values up to +2.05‰ were found in altered basalts, but only when a significant fraction of Fe had been leached. Conversely, $\delta^{57}Fe$ values reaching −2.49‰ were documented in hydrothermal deposits, suggesting that Fe isotopes are susceptible to alteration at high temperature and in samples with notable Fe-loss. Williams et al. (2009) presented $\delta^{57}Fe$ compositions of altered dikes from ODP Hole 504B ranging from 0.10 ± 0.07‰ to 0.33 ± 0.13‰, which do not display the extreme variation seen by Rouxel et al. (2003), likely because these samples did not experience significant Fe-loss. The DSDP Hole 504B dikes extend to slightly heavier values than the MORB average ($\delta^{57}Fe = 0.14 \pm 0.06$‰; Weyer and Ionov, 2007), which supports the notion that ocean crust alteration can result in heavier Fe isotope compositions. This is consistent with experimental work indicating that mineral dissolution preferentially releases light Fe (Brantley et al., 2004; Rouxel et al., 2003; Wiederhold et al., 2006). Furthermore, a recent study of ancient komatiites concluded that most of the Fe isotope fractionation observed was due to alteration (Dauphas et al., 2010) and caution should therefore be used when interpreting Fe isotope compositions of ancient materials. At first glance, it appears that $\delta^{51}V$ may be more robust to alteration versus Fe isotopes. However, a direct comparison requires $\delta^{51}V$ measurement of both low and high temperature alteration products and secondary minerals.

5.2. Fractionation during magma generation and evolution

There is conflicting evidence for the existence of redox-sensitive transition metal isotope fractionation due to partial melting and magmatic differentiation. It is well documented that heavy Fe isotopes preferentially enter the melt phase and that melt evolution drives Fe isotope compositions to still heavier values (e.g., Dauphas et al., 2009; Hibbert et al., 2012; Schoenberg and von Blanckenberg, 2006; Schuessler et al., 2009; Teng et al., 2008; Weyer et al., 2005; Weyer and Ionov, 2007; Williams et al., 2005, 2009). In contrast, there is thus far a lack of resolvable Cr stable isotope fractionation between peridotite and basalt (Schoenberg et al., 2008), despite the change in oxidation state from Cr^{3+} in the mantle to Cr^{2+} in basaltic melts (e.g., Berry et al., 2006). We are not aware of any systematic investigation of the effect of magmatic differentiation on stable Cr isotopes.

We use two sample suites to evaluate the effects of partial melting and differentiation on vanadium isotopes. (1) We examine the peridotitic residues of melting that have experienced a range of melt depletion from fertile compositions to ~30% depletion. (2) We investigate mafic mantle melts including tholeiites from the Reykjanes peninsula, Iceland, basaltic lavas from the Shatsky Rise, Pacific Ocean, and previously published USGS standards BCR2, BIR1a, and BHVO1, 2.

5.2.1. Vanadium isotope composition of peridotites

The peridotites in this study include some of the most melt-depleted material recovered by ocean drilling programs (~20–30%, Bach et al., 2004; Harvey et al., 2006) to fertile continental xenoliths (Ionov, 2004; Ionov and Hofmann, 2007; Ionov et al., 1993, 2005) similar in chemical composition to primitive mantle (e.g., McDonough and Sun, 1995; Palme and O'Neill, 2003). The challenge in working with peridotites from oceanic settings is disentangling secondary effects from the consequences of melt extraction. However, we have demonstrated that $\delta^{51}V$ is generally immune to common alteration processes (Section 5.1). The vanadium contents of our peridotites span an order of magnitude from 11 to 109 $\mu g\,g^{-1}$. A conventional way to express fertility is to use co-variation plots of Al_2O_3 content as a proxy for melt depletion because aluminium is relatively immobile during seafloor weathering (Snow and Dick, 1995) and is insoluble in seawater (Janecky and Seyfried, 1986).

The moderately incompatible behaviour of vanadium is indicated by the significant inverse V–MgO correlation in abyssal peridotites (Niu, 2004) and is confirmed by the positive correlation of V and Al_2O_3 (Fig. 4) as well as correlation of V with different melt extraction indices for residual peridotites in the literature (e.g. Ionov et al., 2006; Lee et al., 2003). It must be kept in mind that our samples span global locations and are from different tectonic settings, which accounts for some scatter. Vanadium isotopes show a reasonable positive correlation with V content (Fig. 5a). Our evaluation of seafloor weathering on highly altered dredged abyssal peridotites (Section 5.1.2) suggested that the heaviest sample (PROT 40D-54) was likely affected by alteration. The next heaviest dredged peridotite (Vulcan 5 41-55) also falls off the correlation between V content and $\delta^{51}V$, and we suggest it has experienced secondary modification and do not consider it further. With the exclusion of the two heaviest dredged abyssal peridotites, there is a positive correlation between $\delta^{51}V$ and Al_2O_3 content (Fig. 5b) yielding an r^2 of 0.4 for V and 0.5 for Al_2O_3 which, given the >20 measurements, equates to less than 8% and 2%, respectively, probability that $\delta^{51}V$, V and Al_2O_3 are uncorrelated. If the positive correlation between $\delta^{51}V$ and Al_2O_3 is taken as a melt extraction trend, it suggests that, like Fe, heavy vanadium preferentially enters the melt and

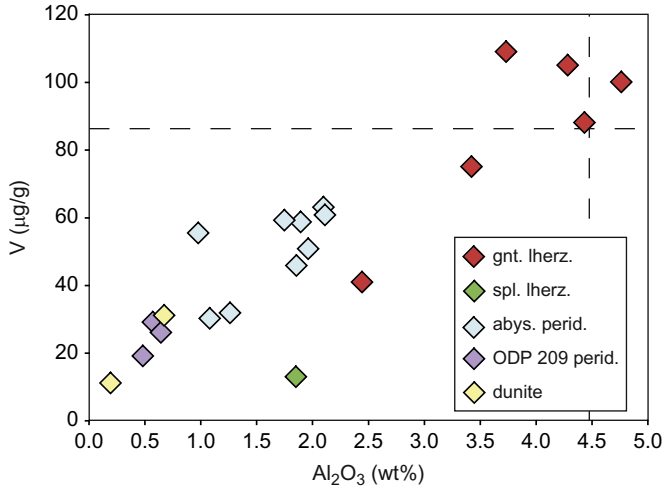

Fig. 4. Variation of Al_2O_3 wt% and V µg g^{-1} for peridotites from this study. The dashed lines are representative of primitive mantle V and Al_2O_3 contents (McDonough and Sun, 1995; Palme and O'Neill, 2003). (The reader is referred to the web version of this article for coloured symbols.)

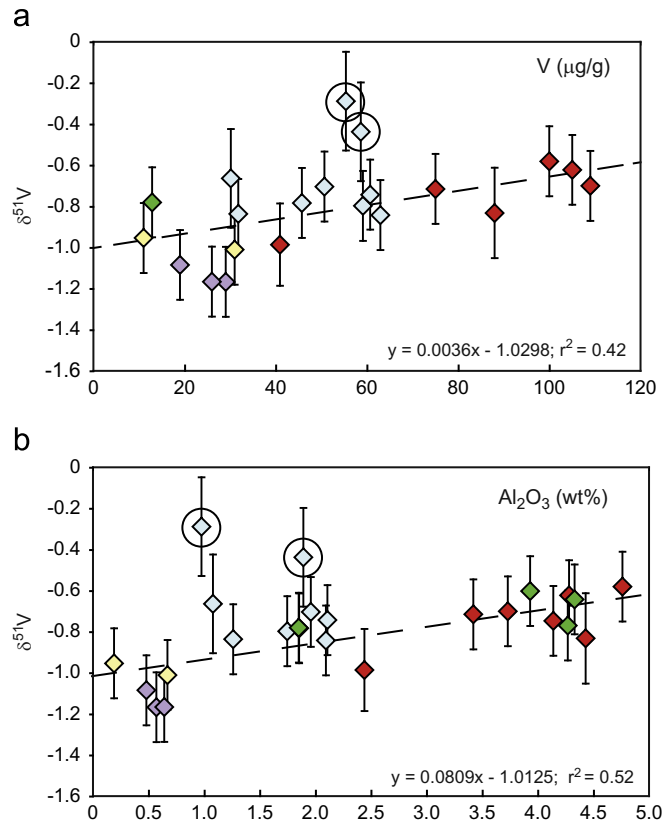

Fig. 5. Stable vanadium isotope composition of peridotites versus (a) V µg g^{-1} and (b) Al_2O_3 wt%. Two circled abyssal peridotites are likely altered (see text) and not included in the linear regression (dashed line). (Symbols as in Fig. 4).

residual peridotites become progressively lighter with increasing extent of melt depletion. However, MORB glass is significantly *lighter* than fertile peridotites ($\delta^{51}V_{MORB} = -0.95 \pm 0.11$‰ 2sd, Fig. 5). A *t*-test of the two groups of measurements (MORB glass and fertile peridotites) indicates that there is only a 0.007% chance that the two groups are from the same population. If the trends in Fig. 5 are due to melt extraction, this would imply that MORB is derived from a largely harzburgitic source region. This is difficult to reconcile with current models of the composition of the MORB sources in the upper mantle (e.g., Salters and Stracke, 2004). Therefore it seems unlikely that partial melting can explain all the observed $\delta^{51}V$ variation in unaltered peridotites.

Alternatively, the $\delta^{51}V$ variation might be explained by equilibrium inter-mineral and mineral–melt isotope fractionation. The major host phases for vanadium in fertile peridotites are, in order of importance, clinopyroxene (cpx), orthopyroxene (opx) and garnet (e.g., Ionov, 2004). There is negligible V in olivine (~1–4 ppm) and it can thus be ignored. Likewise, limited data suggests that vanadium does not strongly partition into sulphides (e.g., Gaetani and Grove, 1997). Vanadium abundance in spinel will be dependent on composition, but are unlikely to have higher concentrations than pyroxene and garnet. Considering the low modal abundance of spinel compared to pyroxene, it follows that V is largely hosted in pyroxenes in both garnet and spinel lherzolites.

Table 2 illustrates the range of whole rock (WR) V contents that can be achieved using the highest and lowest modal abundances and V concentrations from fertile peridotites. In particular, spinel lherzolite concentrations can be reproduced without considering the V budget of spinel. If the relationship between $\delta^{51}V$ and Al_2O_3 (Fig. 5b) is due to equilibrium inter-mineral fractionations, which may affect residue/melt partition coefficient during partial melting, then it requires large isotopic differences between mineral phases. For example, the modal abundance of cpx versus opx changes with melt extraction. However, our dataset provides no evidence for significant $\delta^{51}V$ differences between residual peridotites within a broad cpx/opx range, and hence suggests limited $\delta^{51}V$ fractionation between opx and cpx (Fig. 6). There is also little evidence suggesting a role for $\delta^{51}V$ fractionation due to cpx composition since V concentrations are similar, for example, in coexisting high and low sodium cpx (Ionov et al., 2006).

Equilibrium inter-mineral fractionations are theoretically driven by differences in bonding environment. In general, the stronger bonds formed in lower coordination environments favour isotopically heavy compositions (e.g., Bigeleisen and Mayer, 1947; Schauble et al., 2001). For example, recent study on stable Mg isotopes by Li et al. (2011) use coordination number to explain isotopically light Mg isotopes in garnet (8) versus pyroxene (6). However, this is unlikely to be the case with respect to vanadium in garnet versus pyroxene. Vanadium is octahedrally coordinated in garnet, entering the B site of the general formula $A_3B_2Si_3O_{12}$. There even exists a vanadium end-member of calcium

Table 2
Mineral hosts of vanadium in fertile lherzolites.

Mineral	Modal abundance		V (µg/g^{-1})	V (µg/g^{-1})
	Highest	Lowest	Highest	Lowest
Garnet lherzolite				
Opx	0.212	0.121	113	113
Cpx	0.158	0.111	350	330
Ol	0.633	0.556	4	1
Garnet	0.134	0.086	104	97
WR calculated, V (µg g^{-1})			**82**	**52**
Spinel lherzolite				
Opx	0.311	0.17	111	111
Cpx	0.188	0.016	281	225
Ol	0.777	0.581	4	1
Spinel	0.022	0.007		
WR calculated, V (µg g^{-1})			**90**	**24**

Modal abundances and concentrations from Ionov (2004), except olivine V concentration from Ionov et al. (2006).
WR=whole rock.

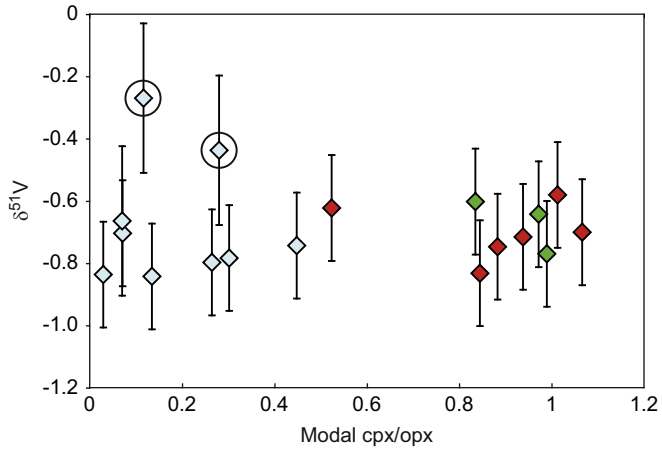

Fig. 6. Stable vanadium isotope composition versus modal ratio of cpx/opx in peridotites. Two altered abyssal peridotites (see text) are circled.

garnet, called Goldmandite, that can contain >4–5 wt% V_2O_3 (e.g., Deer et al., 1966; Moench and Meyrowitz, 1964). Vanadium is also octahedrally coordinated in both clino- and orthopyroxene, entering the M1 site in the general formula $M2M1Si_2O_6$ and some varieties of aegirine–augites can contain >3 wt% V_2O_3 where V^{3+} substitutes for Fe^{3+} (e.g., Deer et al., 1966).

Whilst we cannot further evaluate the role of pyroxenes and garnet with the current whole rock dataset, we can perform a preliminary evaluation of spinel mineral/melt fractionation. Spinel structures are of interest as vanadium and can be either octahedrally or tetrahedrally coordinated and exist dominantly as V^{4+} and V^{5+} (e.g., Toplis and Corgne, 2002). Prytulak et al. (2011) documented evidence for spinel mineral/melt fractionation by employing two different dissolution methods for USGS dunite standard PCC1, finding that samples with residual spinel were isotopically lighter than fully dissolved samples. We purposefully tested this phenomenon by hotplate and bomb dissolutions (Section 3.1) for two extremely depleted and serpentinised harzburgites (Table 1). Lighter $\delta^{51}V$ in samples with residual spinel was again observed, suggesting that spinel is isotopically heavy in these samples. This is in general agreement with the prediction that heavier signatures occur in lower coordination environments. With only analyses from very depleted material (i.e. mostly chromite), we cannot evaluate if there is any isotopic difference linked to spinel composition.

Clearly, pyroxene, garnet and, to a lesser extent, spinel mineral/melt fractionation factors are needed to understand the $\delta^{51}V$ signature of peridotites. The analyses of these mineral phases is analytically tractable, but beyond the scope of this paper.

5.2.2. *Vanadium isotope composition of 'OIB' lavas*

We now compare the $\delta^{51}V_{MORB}$ with mafic material derived from more geochemically enriched sources. These include a suite of tholeiites from Iceland, glassy basalts from the Shatsky Rise large igneous province, and previously published USGS standards BCR2 (Columbia River Basalt), BIR1a (Iceland), and BHVO1 and 2 (Hawaii) from Prytulak et al. (2011).

We first assess the effects of moderate degrees of magmatic differentiation with tholeiites from the Reykjanes peninsula, Iceland. We emphasize that, although the Reykjanes samples are not strictly co-genetic, they are contemporaneous, sparsely phryic ($<5\%$), and have limited variation in radiogenic Sr and Nd isotopes (Peate et al., 2009). We focus on high MgO lavas in keeping with our goal of evaluating $\delta^{51}V$ in the bulk silicate Earth. Determination of $\delta^{51}V$ during evolution to more felsic compositions is beyond the scope of the study. Vanadium correlates with MgO (12.3–6.5 wt%, not shown) in the Rekyjanes tholeiites, however, $\delta^{51}V$ shows no corresponding correlation (Fig. 7a) indicating that differentiation at high MgO does not impact the $\delta^{51}V$ of mafic melts.

Glassy basalts from the Shatsky Rise large igneous province in the Pacific Ocean may have a more geochemically enriched source than MORB. Three of the lavas group tightly together to heavier isotope compositions (-0.68 ± 0.04‰) than MORB (Fig. 7a, b). However, the remaining Shatsky basalt is the lightest sample in the study at $\delta^{51}V=-1.29$‰, albeit with a large error of 0.31‰ 2sd. This lava type was volumetrically minor in the recovered material and is characterized by significant enrichment in incompatible elements, niobium (Nb) in particular (Sano et al., 2012). It is difficult to assess the importance of this isotope signature without further data from similarly enriched lavas. Overall, with the exception of the high-Nb basalt from the Shatsky Rise, no resolvable $\delta^{51}V$ isotope fractionation is seen within all the 'OIB' mafic melts presented in this study (Fig. 7a, b) and they yield an average of $\delta^{51}V'_{OIB}=-0.87\pm0.29$‰ 2sd ($n=17$).

A few observations on the general $\delta^{51}V$ homogeneity in terrestrial basaltic lavas are worth summarizing. (1) There is no $\delta^{51}V$ difference between MORB from ridge systems in the Pacific, Indian and northern Atlantic ocean basins. (2) The admittedly limited dataset of $\delta^{51}V'_{OIB}$ overlaps with MORB, with some Shatsky Rise basalts displaying slightly heavier values. (3) There is no $\delta^{51}V$ fractionation associated with magmatic differentiation at high (>5 wt%) MgO contents.

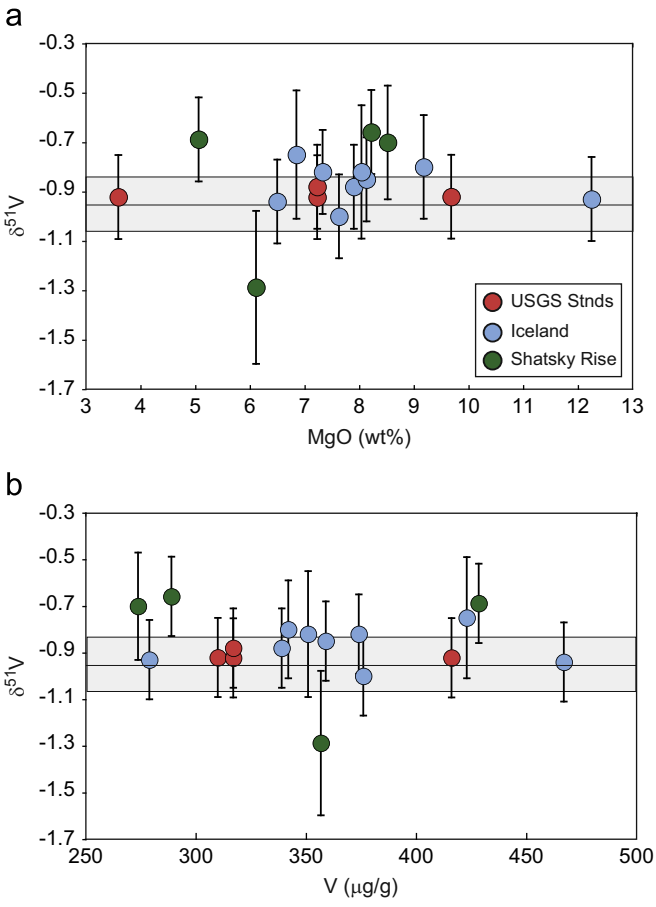

Fig. 7. Stable vanadium isotopes of 'OIB' lavas versus (a) MgO wt% and (b) V $\mu g\,g^{-1}$. Grey box is the range for $\delta^{51}V_{MORB}$.

5.3. $\delta^{51}V$ in terrestrial reservoirs and the bulk silicate Earth

A 'Bulk Silicate Earth' (BSE) value is frequently sought to characterize stable isotope systems (e.g., Pogge von Strandmann et al., 2011; Savage et al., 2010; Schoenberg et al., 2008; Teng et al., 2010; Weyer et al., 2005). The motivation is to pinpoint an 'Earth' value that can be used to compare with extra-terrestrial material, provide information on planetary processes, and define a baseline for future terrestrial organic and inorganic studies.

We have documented a restricted range of $\delta^{51}V$ in basaltic melts and systematic variation in melting residues. Average values for terrestrial reservoirs and the meteoritic range of vanadium isotopes (Nielsen et al., 2011b; Prytulak et al., 2011) are compared in Fig. 8. It should be noted that we do not consider the continental crust. Simple mass balance calculations performed using a V content of 138 $\mu g\,g^{-1}$ in the bulk crust (Rudnick and Gao, 2003) with a mass of 2.25×10^{25} g compared to 82 $\mu g\,g^{-1}$ V (McDonough and Sun, 1995) in the primitive mantle with a mass of 4.00×10^{27} g indicate that less than 1% of the Earth's vanadium is housed in the bulk continental crust and therefore should not significantly impact $\delta^{51}V_{BSE}$. Vanadium is present in the Earth's core, but it is not relevant for bulk silicate Earth calculations.

We employ two approaches to determine $\delta^{51}V_{BSE}$. (1) Use the correlation of $\delta^{51}V$ with V and Al_2O_3, extrapolating the $\delta^{51}V$ to that corresponding to primitive mantle V and Al_2O_3 values. (2) Use a fertile peridotite average (e.g., Pogge von Strandmann et al., 2011). Vanadium in the primitive mantle is estimated at ~82–86 $\mu g\,g^{-1}$ using a combination of data from peridotites and komatiites in addition to correlative relationships between MgO, Ca, Sc, Yb and V (McDonough and Frey, 1989; McDonough and Sun, 1995; Palme and O'Neill, 2003). Using the relationship in Fig. 5a, and V=84 $\mu g\,g^{-1}$ we extrapolate to $\delta^{51}V_{BSE}=-0.7$‰. Robust estimates for Al_2O_3 in the primitive mantle are 4.45 ± 0.44 wt%, (McDonough and Sun, 1995), and 4.49 ± 0.37 wt% (Palme and O'Neill, 2003). Extrapolating to a primitive mantle Al_2O_3 content of 4.47 wt% also yields $\delta^{51}V_{BSE}=-0.7$‰. Finally, if we consider peridotite samples with V > 75 $\mu g\,g^{-1}$ and ≥ 3.5 wt% Al_2O_3 as 'fertile' and average these eight samples (Table 1), we obtain $\delta^{51}V_{BSE}=-0.7\pm0.2$‰ 2sd. Given the agreement between the fertile peridotite average and the extrapolated values from both Al_2O_3 and V, we suggest that $\delta^{51}V_{BSE}=-0.7\pm0.2$‰ 2sd is the current best estimate for the bulk silicate Earth.

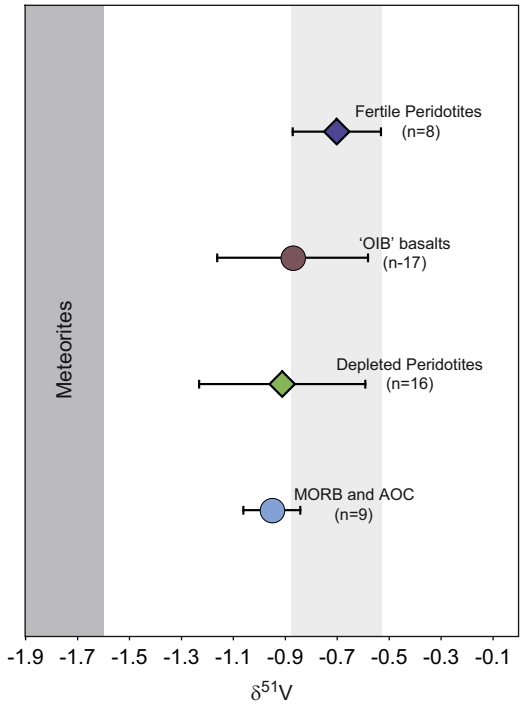

Fig. 8. Stable vanadium isotope composition of terrestrial reservoirs. The grey box is the range measured in meteorites ($\delta^{51}V=-1.6$‰ to −1.9‰; Nielsen et al., 2011b; Prytulak et al., 2011).

6. Summary and outlook

We have presented the first precise stable vanadium isotope measurements of an extensive set of mantle peridotites and mantle-derived mafic rocks, allowing a glimpse into the magnitude of natural isotope fractionation produced at high temperatures and resulting from common alteration processes. Alteration of peridotites and basalts does not appear to induce large vanadium isotope fractionations, although systematic studies of hydrothermal deposits and secondary minerals are still needed. Within the dataset, MORB from different ocean basins show no resolvable vanadium isotopic fractionations, nor are there significant differences between our limited 'OIB' and MORB datasets. However, further investigation of OIB with varying degrees of geochemical enrichment is needed to substantiate these initial observations and explore the hints of isotope variation displayed by, for example, the Shatsky Rise lavas.

The average $\delta^{51}V_{MORB}$ (-0.95 ± 0.11‰ 2sd) and $\delta^{51}V'_{OIB}$ (-0.87 ± 0.29‰ 2sd) overlap with depleted peridotites (Fig. 8). However, residual peridotites that have greater extents of melt depletion display progressively lighter isotope compositions. Given that $\delta^{51}V_{MORB}$ is offset to lighter values than fertile peridotites, it is difficult to reconcile the trend with fractionation during partial melting. The investigation of mineral/melt fractionation factors is critical to fully understand the isotope signatures of bulk peridotities.

We use the average of eight fertile unmetasomatized peridotites with ≥ 3.5 wt% Al_2O_3 and > 75 $\mu g\,g^{-1}$ V as an estimate of the vanadium isotope composition of the bulk silicate Earth ($\delta^{51}V_{BSE}=-0.7\pm0.2$‰). The $\delta^{51}V_{BSE}$ value emphasizes and confirms the significant isotope difference between terrestrial and extra-terrestrial material (Nielsen et al., 2011b; Prytulak et al., 2011, Fig. 8).

The apparent robustness of vanadium isotopes to common alteration processes makes it a potentially powerful tool for the study of ancient mantle and mantle-derived melts. A remaining fundamental question, however, is how vanadium isotope fractionation is related to oxidation state and thus the oxygen fugacity of the system. Investigation of subduction-related lavas and comparison with the tightly defined $\delta^{51}V_{MORB}$ should yield some insight. Given the resolvable isotope fractionation observed at high temperatures, significant potential exists to use stable vanadium isotopes in low temperature environments where isotope fractionation is expected to be even larger.

Acknowledgements

This research used samples provided by the Ocean Drilling Program (ODP) and the Integrated Ocean Drilling Program (IODP). Shipboard support for JP was provided by NERC grant NE/H010319/1 and she thanks the IODP and Transocean/Sedco-Forex staff on board the *JOIDES Resolution* for their contributions to a successful expedition. We acknowledge reviews by F.Z. Teng, O. Rouxel and an anonymous reviewer that improved the manuscript. JP was supported by Petrobras and ERC funding to ANH and

NERC postdoctoral fellowship NE/H01313X/1. SGN was supported by a NERC postdoctoral fellowship. We are grateful to K.W. Burton for providing the Indian Ocean MORB glass. Barry Coles (Imperial) and Nick Belshaw (Oxford) are thanked for instrument support.

Appendix A. Supplementary Information

Supplementary data associated with this article can be found in the online version at http://dx.doi.org/10.1016/j.epsl.2013.01.010.

References

Bach, W., Garrido, C.J., Paulick, H., Harvey, J., Rosner, M., 2004. Seawater–peridotite interactions: first insights from ODP Leg 209, MAR 15°N. Geochem. Geophys. Geosyst. 5, Q09F26, http://dx.doi.org/10.1029/2004GC000744.

Bekker, A., Barley, M.E., Fiorentini, M.L., Rouxel, O.J., Rumble, D., Beresford, S.W., 2009. Atmospheric sulfur in Archean komatiite-hosted nickel deposits. Science 326, 1086–1089.

Bellenger, J.P., Wichard, T., Kutka, A.B., Kraepiel, A.M.L., 2008. Uptake of molybdenum and vanadium by a nitrogen-fixing soil bacterium using siderophores. Nat. Geosci. 1, 243–246.

Berry, A.J., Neill, H.S., Scott, D.R., Foran, G.J., Sheley, J.M.G., 2006. The effect of composition on Cr^{2+}/Cr^{3+} in silicate melts. Am. Mineral. 91, 1901–1908.

Bigeleisen, J., Mayer, M.G., 1947. Calculation of equilibrium constants for isotopic exchange reactions. J. Chem. Phys. 15, 261–267.

Brantley, S.L., Liermann, L.J., Guynn, R.L., Anbar, A., Icopini, G., Barling, J., 2004. Fe isotopic fractionation during mineral dissolution with and without bacteria. Geochim. Cosmochim. Acta 68, 3189–3204.

Canil, D., 1997. Vanadium partitioning and the oxidation state of Archaean komatiite magmas. Nature 389, 842–845.

Chaussidon, M., Albarede, F., Sheppard, S.M.F., 1987. Sulfur isotope heterogeneity in the mantle from ion microprobe measurements of sulfide inclusions in diamonds. Nature 330, 242–244.

Dauphas, N., Craddock, P.R., Asimow, P.D., Bennett, V.C., Nutman, A.P., Ohnenstetter, D., 2009. Iron isotopes may reveal redox conditions of mantle melting from Archean to present. Earth Planet. Sci. Lett. 288, 255–267.

Dauphas, N., Teng, F.-Z., Arndt, N.T., 2010. Magnesium and iron isotopes in 2.7 Ga Alexo komatiites: mantle signatures, no evidence for Soret diffusion, and identification of diffusive transport in zoned olivine. Geochim. Cosmochim. Acta 74, 3274–3291.

Dawson, J.B., Powell, D.G., Reid, A.M., 1970. Ultrabasic xenoliths and lava from the Lashaine volcano, northern Tanzania. J. Petrol. 11, 519–548.

Deer, W.A., Howie, R.A., Zussman, J., 1966. An Introduction to the Rock-Forming Minerals. Longman, London. (528 pp).

Eiler, J.M., Farley, K.A., Valley, J.W., Hofmann, A.W., Stolper, E.M., 1996. Oxygen isotope constraints on the sources of Hawaiian volcanism. Earth Planet. Sci. Lett. 144, 453–468.

Elderfield, H., Schultz, A., 1996. Mid-ocean ridge hydrothermal fluxes and the chemical composition of the ocean. Annu. Rev. Earth Sci. 24, 191–224.

Elkins, L.J., Sims, K.W.W., Prytulak, J., Elliott, T., Mattielli, N., Blichert-Toft, J., Blusztajn, J., Dunbar, N., Devey, C., Mertz, D.F., Schilling, J.-G., Murrell, M., 2011. Understanding melt generation beneath the slow-spreading Kolbeinsey Ridge using ^{238}U, ^{230}Th, and ^{231}Pa excesses. Geochim. Cosmochim. Acta 75, 6300–6329.

Elliott, T., Thomas, A., Jeffcoate, A., Niu, Y., 2006. Lithium isotope evidence for subduction-enriched mantle in the source of mid-ocean-ridge basalts. Nature 443, 565–568.

Emerson, S.R., Huested, S.S., 1991. Ocean anoxia and the concentrations of molybdenum and vanadium in seawater. Mar. Chem. 34, 177–196.

Gaetani, G.A., Grove, T.L., 1997. Partitioning of moderately siderophile elements among olivine, silicate melt, and sulfide melt: constraints on core formation in the Earth and Mars. Geochim. Cosmochim. Acta 61, 1829–1846.

Gannoun, A., Burton, K.W., Parkinson, I.J., Alard, O., Schiano, P., Thomas, L.E., 2007. The scale and origin of the osmium isotope variations in mid-ocean ridge basalts. Earth Planet. Sci. Lett. 259, 541–556.

Halliday, A.N., Stirling, C.H., Freedman, P.A., Oberli, F., Reynolds, B., Georg, R.B. 2010. High precision isotope ratio measurements using multiple collector inductively coupled plasma mass spectrometry. In: Encyclopedia of Mass Spectrometry, vol. 5, Elemental and Isotope Ratio Mass Spectrometry. Elsevier, pp. 242–260 (Chapter 17).

Harvey, J., Gannoun, A., Burton, K.W., Rogers, N.W., Alard, O., Parkinson, I.J., 2006. Ancient melt extraction from the oceanic upper mantle revealed by Re–Os isotopes in abyssal peridotites from the Mid-Atlantic ridge. Earth Planet. Sci. Lett. 244, 606–621.

Hibbert, K.E.J., Williams, H.M., Kerr, A.C., Putchel, I.S., 2012. Iron isotopes in ancient and modern komatiites: evidence in support of an oxidized mantle from Archean to present. Earth Planet. Sci. Lett. 321–322, 198–207.

Hofmann, A.W., 2003. Sampling mantle heterogeneity through oceanic basalts: isotopes and trace elements. In: Treatise on Geochemistry, vol. 2. Elsevier, Oxford, pp. 61-101.

Ionov, D.A., 2004. Chemical variations in peridotite xenoliths from Vitim, Siberia: inferences for REE and Hf behaviour in the garnet facies upper mantle. J. Petrol. 45, 343–367.

Ionov, D.A., Ashchepkov, I.V., Stosch, H.G., Witt-Eickschen, G., Seck, H.A., 1993. Garnet peridotite xenoliths from the Vitim volcanic field, Baikal region: the nature of the garnet–spinel peridotite transition zone in the continental mantle. J. Petrol. 34, 1141–1175.

Ionov, D.A., Ashchepkov, I., Jagoutz, E., 2005. The provenance of fertile off-craton lithospheric mantle? Sr–Nd isotope and chemical composition of garnet and spinel peridotite xenoliths from Vitim, Siberia. Chem. Geol. 217, 41–75.

Ionov, D.A., Chazot, G., Chauvel, C., Merlet, C., Bodinier, J.-L., 2006. Trace element distribution in peridotite xenoliths from Tok, SE Siberian craton: a record of pervasive, multi-stage metasomatism in shallow refractory mantle. Geochim. Cosmochim. Acta 70, 1231–1260.

Ionov, D.A., Hofmann, A.W., 2007. Depth of formation of subcontinental off-craton peridotites. Earth Planet. Sci. Lett. 261, 620–634.

Janecky, D.R., Seyfried, W.E., 1986. Hydrothermal serpentinization of peridotite within the ocean crust: experimental investigations of mineralogy and major element chemistry. Geochim. Cosmochim. Acta 50, 1357–1378.

Kelley, K.A., Plank, T., Ludden, J., Staudigel, H., 2003. Composition of altered oceanic crust at ODP Sites 801 and 1149. Geochem. Geophys. Geosyst. 4, 8910, http://dx.doi.org/10.1029/2002GC000435.

Komor, S., Elthon, D., Casey, J., 1985. Serpentinization of cumulate ultramafic rocks from the North Arm Mountain massif of the Bay of Islands Ophiolite. Geochim. Cosmochim. Acta 49, 2331–2338.

Lee, C.-T., Brandon, A.D., Norman, M., 2003. Vanadium in peridotites as a proxy for paleo-fO_2 during partial melting: prospects, limitations, and implications. Geochim. Cosmochim. Acta 67, 3045–3064.

Lee, C.-T.A., Leeman, W.P., Canil, D., Li, Z.-W.A., 2005. Similar V/Sc systematics in MORB and Arc basalts: implications for the oxygen fugacities of their mantle sources. J. Petrol. 46, 2313–2336.

Li, Z.-X.A., Lee, C.-T.A., 2004. The constancy of upper mantle fO_2 through time inferred from V/SC ratios in basalts. Earth Planet. Sci. Lett. 228 483–493

Li, W.-Y., Teng, F.-Z., Xiao, Y., Huang, J., 2011. High-temperature inter-mineral magnesium isotope fractionation in eclogite from the Dabie orogen, China. Earth Planet. Sci. Lett. 304, 224–230.

Lopez, L., Lomonaco, S., Galarraga, F., Lira, A., Cruz, C., 1995. V/Ni ratio in maltene and asphaltene fractions of crude oils from the west Venezuela basin—correlation studies. Chem. Geol. 119, 255–262.

McDonough, W.F., Frey, F.A., 1989. REE in upper mantle rocks. In: Lipin, B., McKay, G.R. (Eds.), Geochemistry and Mineralogy of Rare Earth Elements. Mineralogical Society of America, Chelsea, Michigan, pp. 99–145.

McDonough, W.F., Sun, S.-s., 1995. The composition of the Earth. Chem. Geol. 120, 223–253.

Moench, R.H., Meyrowitz, R., 1964. Goldmandite, a vanadium garnet from Laguna, New Mexico. Am. Mineral. 49, 644–655.

Nielsen, S.G., Rehkämper, M., Norman, M.D., Halliday, A.N., 2006. Thallium isotopic evidence for ferromanganese sediments in the mantle source of Hawaiian basalts. Nature 439, 314–317.

Nielsen, S.G., Prytulak, J., Halliday, A.N., 2011a. Determination of precise and accurate $^{51}V/^{50}V$ isotope ratios by MC-ICP-MS, Part 1: Chemical separation of vanadium and mass spectrometric protocols. Geostand. Geoanal. Res. 35, 293–306.

Nielsen, S.G., Prytulak, J., Wood, B.J., Halliday, A.N., 2011b. Large vanadium isotope difference between silicate Earth and meteorites. Goldschmidt 2011 abstract volume. Mineral. Mag. 75, 1539.

Niu, Y., 2004. Bulk-rock major and trace element composition of abyssal peridotites: implications for mantle melting, melt extraction and post-melting processes beneath mid-ocean ridges. J. Petrol. 45, 2423–2458.

Palme, H., O'Neill, H. St. C., 2003. Cosmochemical estimates of mantle composition. In: Treatise on Geochemistry, vol. 2. Elsevier, Oxford pp. 1–35.

Peate, D.W., Baker, J., Jakobsson, S.P., Waight, T.E., Kent, A.J.R., Grassineau, N.V., Skovgaard, A.C., 2009. Historic magmatism on the Reykjanes Peninsula, Iceland: a snap-shot of melt generation at a ridge segment. Contrib. Mineral. Petrol. 157, 359–382.

Plank, T., Ludden, J.N., Escutia, C., Abrams, L.J., Alt, J.C., Armstrong, R.N., Barr, S.R., Bartolini, A., Cairns, G., Fisk, M., Guerin, G., Haveman, S.A., Hirono, T., Honnore'z, J., Kelley, K.A., Larson, R.L., Lozar, F.M., Murray, R.W., Pletsch, T.K., Pockalny, R.A., Rouxel, O., Schmidt, A., Smith, D.C., Spivack, A.J., Staudigel, H., Steiner, M.B., Valentine, R.B. 2000. In: Proceedings of the Ocean Drilling Program, Initial Reports, vol. 185. Ocean Drilling Program, College Station, TX.

Pogge von Strandmann, P.A.E., Elliott, T., Marschall, H.R., Coath, C., Lai, Y.-J., Jeffcoate, A.B., Ionov, D.A., 2011. Variations of Li and Mg isotope ratios in bulk chondrites and mantle xenoliths. Geochim. Cosmochim. Acta 75, 5247–5268.

Prytulak, J., Nielsen, S.G., Halliday, A.N., 2011. Determination of precise and accurate $^{51}V/^{50}V$ isotope ratios by multi-collector ICP-MS, Part 2: Isotopic composition of six reference materials plus the Allende chondrite and verification tests. Geostand. Geoanal. Res. 35, 307–318.

Rouxel, O., Dobbek, N., Ludden, J., Fouquet, Y., 2003. Iron isotope fractionation during ocean crust alteration. Chem. Geol. 202, 155–182.

Rudnick, R.L., Gao, S., 2003. Composition of the continental crust. In: Treatise on Geochemistry, vol. 3. Elsevier, Oxford, pp. 1-64.

Sager, W.W., Sano, T., Geldmacher, J., and the Expedition 324 Scientists, 2010. In: Proceedings of the Integrated Ocean Drilling Program, vol. 324, Integrated Ocean Drill Program Management International, Inc. Washington, DC, doi:10.2204/iodp.proc.324.101.2010.

Salters, V.J.M., Stracke, A., 2004. Composition of the depleted mantle. Geochem. Geophys. Geosyst. 5, Q05004, http://dx.doi.org/10.1029/2003GC000596.
Sano, T., Shimizu, K., Ishikawa, A., Senda, R., Chang, Q., Kimura, J.-I., Widdowson, M., Sager, W.W., 2012. Variety and origin of magmas on Shatsky Rise, northwest Pacific Ocean. Geochem. Geophys. Geosyst. 13, Q08010, http://dx.doi.org/10.1029/2012GC004235.
Savage, P.S., Georg, R.B., Armytage, R.M.G., Williams, H.M., Halliday, A.N., 2010. Silicon isotope homogeneity in the mantle. Earth Planet. Sci. Lett. 295, 139–146.
Schauble, E.A., Rossman, G.R., Taylor, H.P., 2001. Theoretical estimates of equilibrium Fe-isotope fractionations from vibrational spectroscopy. Geochim. Cosmochim. Acta 65, 2487–2497.
Schauble, E.A., 2004. Applying stable isotope fractionation theory to new systems. Rev. Mineral. Geochem. 55, 65–111.
Schauble, E.A., Méheut, M., Hill, P.S., 2009. Combining metal stable isotope fractionation theory with experiments. Elements 5, 369–374.
Schoenberg, R., von Blanckenberg, F., 2006. Modes of planetary-scale Fe isotope fractionation. Earth Planet. Sci. Lett. 252, 342–359.
Schoenberg, R., Zink, S., Staubwasser, M., von Blanckenburg, F., 2008. The stable Cr isotope inventory of solid Earth reservoirs determined by double spike MC-ICP-MS. Chem. Geol. 249, 294–306.
Schuessler, J.A., Schoenberg, R., Sigmarsson, O., 2009. Iron and lithium isotope systematics of the Hekla volcano, Iceland—evidence for Fe isotope fractionation during magmatic differentiation. Chem. Geol. 258, 78–91.
Snow, J.E., Dick, H.J.B., 1995. Pervasive magnesium loss by marine weathering of peridotite. Geochim. Cosmochim. Acta 59, 4219–4235.
Staudigel, H., 2003. Hydrothermal alteration processes in the oceanic crust. Treatise on Geochemistry 3.15, pp. 511–535.
Teng, F.-Z., Dauphas, N., Helz, R.T., 2008. Iron isotope fractionation during magmatic differentiation in Kilauea Iki lava lake. Science 320, 1620–1622.
Teng, F.-Z., Li, W.Y., Ke, S., Marty, B., Dauphas, N., Huang, S.C., Wu, F.Y., Pourmand, A., 2010. Magnesium isotopic composition of the Earth and chondrites. Geochim. Cosmochim. Acta 74, 4150–4166.
Teng, F.-Z., Dauphas, N., Helz, R., Gao, S., Huang, S.C., 2011. Diffusion-driven magnesium and iron isotope fractionation in Hawaiian olivine. Earth Planet. Sci. Lett. 308, 317–324.
Toplis, M.J., Corgne, A., 2002. An experimental study of element partitioning between magnetite, clinopyroxene and iron-bearing silicate liquids with particular emphasis on vanadium. Contrib. Mineral. Petrol. 144, 22–37.
Tribovillard, N., Algeo, T.J., Lyons, T., Riboulleau, A., 2006. Trace metals as paleoredox and paleoproductivity proxies: an update. Chem. Geol. 232, 12–32.
Urey, H.C., 1947. The thermodynamic properties of isotopic substances. J. Chem. Soc. (London), 562–581.
Weyer, S., Ionov, D.A., 2007. Partial melting and melt percolation in the mantle: the message from Fe isotopes. Earth Planet. Sci. Lett. 259, 119–133.
Weyer, S., Seitz, H.-M., 2012. Coupled lithium- and iron isotope fractionation during magmatic differentiation. Chem. Geol. 294–295, 42–50.
Weyer, S., Anbar, A.D., Brey, G.P., Munker, C., Mezger, K., Woodland, A.B., 2005. Iron isotope fractionation during planetary differentiation. Earth Planet. Sci. Lett. 240, 251–264.
Wiederhold, J.G., Kraemer, S.M., Teutsch, N., Borer, P.M., Halliday, A.N., Kretzschmar, R., 2006. Iron isotope fractionation during proton-promoted, ligand-controlled, and reductive dissolution of goethite. Environ. Sci. Technol. 40, 3787–3793.
Williams, H.M., McCammon, C.A., Peslier, A.H., Halliday, A.N., Teutsch, N., Levasseur, S., Burg, J.-P., 2004. Iron isotope fractionation and the oxygen fugacity of the mantle. Science 304, 1656–1659.
Williams, H.M., Peslier, A.H., McCammon, C., Halliday, A.N., Levasseur, S., Teutsch, N., Burg, J.-P., 2005. Systematic iron isotope variations in mantle rocks and minerals: the effects of partial melting and oxygen fugacity. Earth Planet. Sci. Lett. 235, 435–452.
Williams, H.M., Nielsen, S.G., Renac, C., Griffin, W.L., O'Reilly, S.Y., McCammon, C.A., Pearson, N., Viljoen, F., Alt, J.C., Halliday, A.N., 2009. Fractionation of oxygen and iron isotopes by partial melting processes: implications for the interpretation of stable isotope signatures in mafic rocks. Earth Planet. Sci. Lett. 283, 156–166.
Wood, B.J., Wade, J., Kilburn, M.R., 2008. Core formation and the oxidation state of the Earth: additional constraints from Nb, V and Cr partitioning. Geochim. Cosmochim. Acta 72, 1415–1426.
Zindler, A., Hart, S., 1986. Chemical geodynamics. Annu. Rev. Earth Planet. Sci. 14, 493–571.
Zhu, X.K., Guo, Y., Williams, R.J.P., O'Nions, R.K., Matthews, A., Belshaw, N.S., Canters, G.W., de Waal, E.C., Weser, U., Burgess, B.K., Salvato, B., 2000. Mass fractionation processes of transition metal isotopes. Earth Planet. Sci. Lett. 200, 47–62.